1 319-nm single-frequency output from diffusion-bonded monolithic nonplanar Nd:YAG ring resonator with undoped end

Mingwei Gao (高明伟)*, Yu Zhao (赵 宇), Luyan Zhang (张路岩), Lei Wang (王 磊), and Chunqing Gao (高春清)

School of Opto-Electronics, Beijing Institute of Technology, Beijing 100081, China

**Corresponding author: ghew@bit.edu.cn*

Received October 12, 2012; accepted December 20, 2012; posted online, 2013

An efficient 1 319-nm Nd:YAG single-frequency laser is demonstrated in a diffusion-bonded nonplanar ring oscillator (NPRO) with an undoped end. The thermal model of diffusion-bonded NPRO is generated to analyze the temperature field and thermal focal length. A stable single-frequency output power of up to 1.55 W is obtained at 1 319 nm.

OCIS codes: 140.3410, 140.3580, 140.6810.

doi: 10.3788/COL201311.041406.

The 1 319-nm single-frequency lasers are used in many different applications, such as laser frequency standards, fiber optic hydrophones, and sodium guide stars. Several methods have been employed to obtain 1 319-nm single-frequency operation in solid-state lasers, such as in a microchip cavity, an etalon inside a cavity, a twisted mode cavity, and a unidirectional ring oscillator. The monolithic nonplanar ring oscillator (NPRO) first reported by Kane *et al.*[1] has the advantages of high stability, narrow linewidth, low frequency and intensity noises, and good beam quality. Nonplanar monolithic ring lasers based on Nd:YAG have been successfully used in many wavelengths, such as 946, 1 064, 1 122, and 1 319 nm[2−5]. However, the oscillation of a single-frequency 1 319-nm laser is much more difficult to achieve compared with a 1 064-nm laser. As the stimulated emission cross-section of 1 319 nm is only 1/5 of that of 1 064 nm in Nd: YAG, the threshold of 1 319-nm oscillation is much higher than that of 1 064 nm with a lower efficiency. In some applications, a higher power for 1 319-nm single-frequency output is necessary. However, for NPROs with resonators composed of a single crystal, the length of the resonator is limited to several tens of millimeters. When the 1 319-nm NPRO laser is operated under high-pump power condition, the laser fundamental transverse mode would be too small to match the beam size of the high-power pump diodes, thus limiting the power scaling possibilities. Different research groups have attempted to reduce the thermal effect of NPRO lasers. By using a negative curved front facet in compensating the thermally induced lensing inside the crystal, mode matching is improved under high-pumping power condition, which leads to a stable 1 319-nm single-frequency output power up to 0.8 W[6]. About 1.4-W single-frequency output is generated from a composite resonator combined with an undoped NPRO resonator with an end-pumped thin-disk laser that has good thermal property in high-power operation[7]. However, most of these lasers suffer from highly complicated manufacturing and imprecise alignment. In this letter, a diffusion-bonded Nd:YAG 1 319-nm NPRO laser is introduced to reduce the thermal lens effect under high-power pumping condition. The beam transverse mode is analyzed according to the temperature distribution calculated by finite element method. The experiment proves that the diffusion-bonded NPRO can achieve a much higher single-frequency output compared with that of the unbonded NPRO.

A schematic diagram of the monolithic diffusion-bonded 1 319-nm Nd:YAG NPRO crystal is shown in Fig. 1. An undoped YAG crystal was used to reduce the thermal effect generated by higher pump power, and was placed in front of the Nd: YAG crystal with 0.8-at.-% doped concentration. The facets containing B, C, and D are optically polished flat surfaces on the Nd:YAG crystal where total internal reflections occur. The output coupler at A is a surface designed to have a high transmission coating at 808 nm and a partial output coupling coating of the s-polarized beam at 1 319-nm. The three total internal reflections create an effect analogous to a rotation by a half-wave plate, and the output coupler acts as a partial polarizer. With a magnetic field, the crystal acts as a Faraday rotator.

The length of the undoped YAG crystal is a very important parameter that determines the temperature distribution of the crystal and the laser gain length. We first built the thermal equation to determine the optimized length of the undoped YAG crystal. In NPRO, the main heat is from the absorption of laser diode pump light in the laser crystal, and the temperature rise leads to the thermal lens effect. The Poisson equation describing the temperature distribution T in the crystal[8] is

$$\nabla^2 T(r_0, z) = -\frac{Q(r,z)}{K} = \frac{\partial^2}{\partial r^2} T(r,z) + \frac{1}{r}\frac{\partial}{\partial r} T(r,z), \quad (1)$$

where K is the heat conductivity of YAG and $Q(r, z)$ is the heat source density. In NPRO, a rectangular coordinate is more suitable, so the Poisson equation can be expressed as

$$-\frac{Q(x,y,z)}{K} = \frac{\partial^2 T}{\partial^2 x} + \frac{\partial^2 T}{\partial^2 y} + \frac{\partial^2 T}{\partial^2 z}, \quad (2)$$

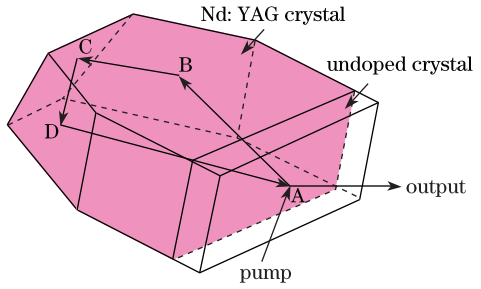

Fig. 1. Diffusion-bonded Nd:YAG NPRO crystal.

$$Q(x,y,z) = \frac{2\eta p}{\pi w_{\mathrm{p}}^2[1-\exp(-\alpha l)]} \times \exp\left[\frac{-2(x^2+y^2)}{w_{\mathrm{p}}^2} - \frac{\alpha(z-d)}{\cos\theta}\right], \quad (3)$$

where η is the pump efficiency, d is the thickness of undoped YAG end, p is the pump power, θ is the incident angle, α is the absorption factor, w_{p} is the $1/e^2$ Gaussian radius of the pump beam (we assume that w_{p} does not vary significantly over the length of the pumped region in the rod), and l is the length of the doped medium. Using Eqs. (2) and (3), we can calculate the temperature distribution in the crystal.

By definite element method, the temperature field distribution of the unbonded NPRO shown in Fig. 2(a) was obtained. For comparison, the temperature field distribution of the diffusion-bonded NPRO with an undoped YAG segment is shown in Fig. 2(b). The peak temperature of the bonded crystal is lower than that of the unbonded crystal. Furthermore, the peak temperature point appearing inside the crystal rather than on the front surface facilitates the reduction of the surface thermal distortion that considerably impacts beam quality.

The inhomogeneous temperature distribution inducing optical path difference ΔOPD is the main cause of the thermal lensing effect. By ignoring the end-face curvature and the thermal-induced strain, the proximate expression of ΔOPD can be obtained as[9]

$$\Delta\mathrm{OPD}(r,z) = \int_d^l \frac{\mathrm{d}n}{\mathrm{d}T}\cdot\Delta T(r,z)\mathrm{d}z,$$
$$\Delta T(r,z) = T(r,z) - T_0, \quad (4)$$

where r is the radial coordinate, z is the axis coordinate, $\mathrm{d}n/\mathrm{d}T$ is the change of the refractive index with temperature, $T(r,\ z)$ is the temperature in the media, d is the width of the undoped YAG, l is the whole crystal length, and T_0 is the constant boundary temperature.

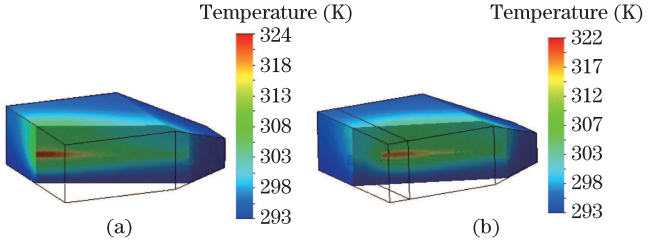

Fig. 2. (Color online) Temperature distribution in NPRO with (a) no undoped end and (b) 1-mm undoped end.

ΔOPD(0,0) is the optical path difference in the laser material center, where the thermal focal length f_{th} can be written as

$$f_{\mathrm{th}} = -\frac{r^2}{2\cdot[\Delta\mathrm{OPD}(r,z) - \Delta\mathrm{OPD}(0,0)]}. \quad (5)$$

From Fig. 3, the thermal focal length in the diffusion-bonded NPRO rapidly decreases compared with the length of the undoped region. The thermal focal length almost remains constant at its minimum when the length of the undoped part is larger than 2 mm and has a pump power from 2 to 6 W. The increase in diffusion bonding width is at the expense of gain length, so the optimized width of diffusion bonding is chosen as 2 mm.

According to the theory of Gaussian beam, the laser mode width strongly depends on the focal length of the thermally induced lens. The fundamental beam radius w_0 can be obtained as

$$w_0 = \sqrt{\lambda/\pi}\cdot\left(L\cdot f_{\mathrm{th}} - \frac{L^2}{4}\right)^{1/4}, \quad (6)$$

where L is the length of the resonant cavity and λ is the laser wavelength. Prior knowledge stated that smaller f_{th} suppressed w_0 better, as shown in Fig. 4.

In Fig. 4, fundamental beam width is shown as a function of pump power. A diode laser with an emitting aperture of 100 μm was used as pump source. A 1× image system is used to focus the pump light into the NPRO, which corresponds to a pump beam width at the edge of the absorption zone of 110 μm when the aberration of the focus system is considered. Thus, to achieve

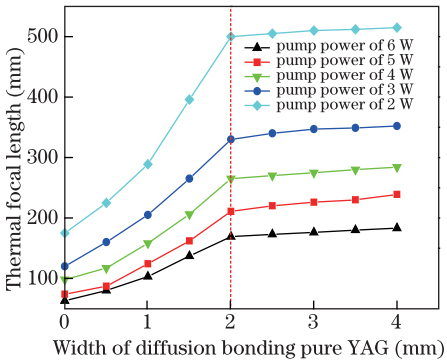

Fig. 3. Thermal focal lengths of NPRO versus thickness of undoped cell at different pump powers.

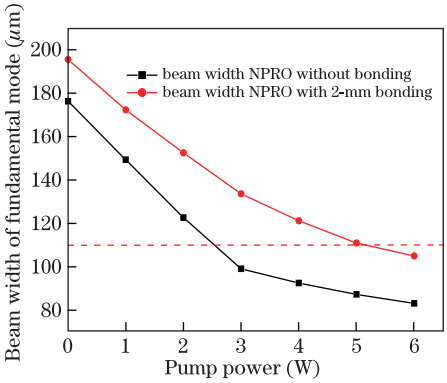

Fig. 4. Laser beam waist w_0 versus pump power.

fundamental mode resonation of the NPRO laser, its fundamental mode width has to be larger than this value. For a NPRO laser without bonding, a fundamental mode width of more than 110 μm is obtained only for pump powers below 2.6 W. For comparison, pump power up to 5 W was applied, which indicates a greater single-frequency power output.

To estimate the property of the diffusion-bonded Nd:YAG NPRO, experiments comparing them with unbonded NPRO were conducted. To minimize the thermal effect, the width of the bonding part was set as 2 mm. The pump source was an 808-nm fiber-coupled diode laser with a core diameter of 100 μm and a numerical aperture of 0.22. Two focusing lenses with 25-mm focal length were used to focus the pump beam into the laser crystal. Two NPRO crystals were equally designed to have a high-transmission coating at 808 nm and a 2% output coupling coating of the s-polarized beam at 1 319 nm. To achieve unidirectional oscillation, a magnetic field of 0.3 T was applied along the Nd:YAG NPRO. The temperature of the two NPRO crystals was controlled at 25 °C by using a thermal electric cooler. From Fig. 5, maximum single-frequency output power of 1.55 W for the bonded NPRO laser was obtained with a 5.2-W pump power, with a slope efficiency of 25%. By contrast, a maximum single-frequency output power of 0.66 W for the unbonded NPRO laser was achieved. Further increase in the pump power caused a multimode oscillation, which agreed with the theoretical analysis. In Fig. 6, a typical longitudinal spectrum of the single-frequency laser of diffusion-bonded NPRO laser at 1.55-W output power was obtained by a scanning Fabry–Perot interferometer with a free spectral region of 3.75 GHz and a finesse of about 100. The 1.319-μm output wave of

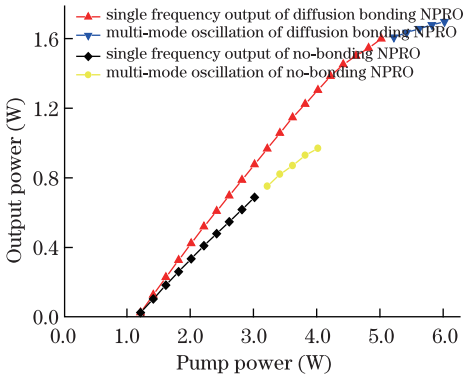

Fig. 5. Output power versus incident pump power.

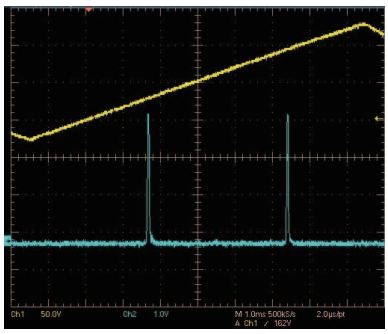

Fig. 6. Longitudinal spectrum of the single frequency.

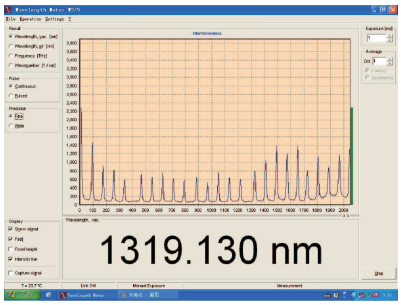

Fig. 7. Longitudinal spectrum of the single-frequency laser of the diffusion-bonded NPRO.

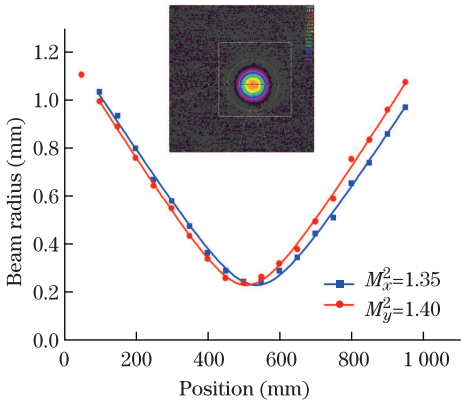

Fig. 8. Beam spot profile and beam quality.

the Nd:YAG-bonded NPRO observed with a wavemeter (HighFinesse WS/5) is shown in Fig. 7. In Fig. 8, the 2D beam profile and beam quality of the single-frequency laser at 1.55-W output power measured by Spiricon PY-III is shown.

In conclusion, a thermal model of the diffusion-bonded NPRO is built to analyze the temperature field and the thermal focal length. Compared with the unbonded NPRO, the diffusion-bonded part can efficiently reduce the temperature and the thermal lens effect. We demonstrate good single-frequency operation in a diode-pumped diffusion-bonded Nd:YAG NPRO. Up to 1.55 W stable single-frequency output at 1.319 μm is obtained with a slope efficiency of 40%.

References

1. T. J. Kane, A. C. Nilsson, and R. L. Byer, Opt. Lett. **12,** 175 (1987).
2. K. Gong, K. Wu, S. He, and Y. Huo, Chinese J. Lasers (in Chinese) **36,** 1719 (2009).
3. H. Zimer and U. Wittrock, Opt. Lett. **29,** 1635 (2004).
4. C. Gao, L. Zhu, R. Wang, M. Gao, Y. Zheng, and L. Wang, Opt. Lett. **37,** 1869 (2012).
5. C. Gao, M. Gao, Y. Zhang, Z. Lin, and L. Zhu, Opt. Lett. **34,** 3029 (2009).
6. I. Freitag, A. Tünnermann, and H. Welling, Opt. Commun. **115,** 511 (1995).
7. D. W. Hughes, M. W. Phillips, J. R. M. Barr, and D. C. Hanna, IEEE J. Quantum Electron. **28,** 1010 (1992).
8. P. J. Hardman, W. A. Clarkson, G. J. Friel, M. Pollnau, and D. C. Hanna, IEEE J. Quantum Electron. **35,** 647(1999).
9. W. A. Clarkson, Appl. Phys. **34,** 2381 (2001).